

Cite this: *Chem. Sci.*, 2021, 12, 8252

All publication charges for this article have been paid for by the Royal Society of Chemistry

# Alkylsulfenyl thiocarbonates: precursors to hydropersulfides potently attenuate oxidative stress†

Vinayak S. Khodade,<sup>‡a</sup> Sahil C. Aggarwal,<sup>‡a</sup> Blaze M. Pharoah,<sup>a</sup> Nazareno Paolucci<sup>bc</sup> and John P. Toscano<sup>id</sup> \*<sup>a</sup>

The recent discovery of the prevalence of hydropersulfides (RSSH) species in biological systems suggests their potential roles in cell regulatory processes. However, the reactive and transient nature of RSSH makes their study difficult, and dependent on the use of donor molecules. Herein, we report alkylsulfenyl thiocarbonates as a new class of RSSH precursors that efficiently release RSSH under physiologically relevant conditions. RSSH release kinetics from these precursors are tunable through electronic modification of the thiocarbonate carbonyl group's electrophilicity. In addition, these precursors also react with thiols to release RSSH with a minor amount of carbonyl sulfide (COS). Importantly, RSSH generation by these precursors protects against oxidative stress in H9c2 cardiac myoblasts. Furthermore, we demonstrate the ability of these precursors to increase intracellular RSSH levels.

Received 17th March 2021

Accepted 14th May 2021

DOI: 10.1039/d1sc01550h

rsc.li/chemical-science

## Introduction

Recently, hydrogen sulfide (H<sub>2</sub>S) has been reported to exert several favorable physiological effects including vasorelaxation, inhibition of myocardial ischemia-reperfusion injury, and slowing the development of atherosclerosis.<sup>1–3</sup> Many of the biological effects of H<sub>2</sub>S have been attributed to the formation of hydropersulfide (RSSH) species.<sup>4–6</sup> Indeed, recent studies have demonstrated that RSSH species such as cysteine hydropersulfide (Cys-SSH) and glutathione hydropersulfide (GSSH) are endogenously produced at significant levels in various organisms, including mammals.<sup>7,8</sup> Furthermore, cysteine residues in a variety of proteins and enzymes have been reported to be modified to the corresponding hydropersulfides.<sup>9,10</sup> The chemical properties and abundance of these species suggest that RSSH play important roles in various physiological processes.<sup>11</sup> CysSSH can be generated *via* the enzymes cystathionine  $\gamma$ -lyase (CSE) and cystathionine  $\beta$ -synthase (CBS), both of which utilize cystine (CysSSCys) as a substrate.<sup>7,12</sup> In addition, recently it has been reported that CysSSH can be synthesized by cysteinyl-tRNA synthetases (CARs) utilizing CysSH as a substrate.<sup>13</sup> The reaction of H<sub>2</sub>S with oxidized thiols

such as disulfides (RSSR) and sulfenic acids (RSOH) can also generate RSSH.<sup>14</sup> Despite these findings, the physiological functions of RSSH remain poorly understood.

RSSH species possess unique chemical properties that are not found in other biologically relevant sulfur species. For instance, RSSH are significantly more nucleophilic than their thiol (RSH) counterparts, likely due to the alpha effect.<sup>14–16</sup> Additionally, RSSH have been proposed to behave as potent antioxidants and may play an important role in maintaining the cellular redox balance.<sup>17</sup> The high nucleophilicity of RSSH can result in the efficient scavenging of reactive electrophiles. Recently, Fukuto and co-workers have reported that increased levels of intracellular RSSH exhibit enhanced resistance to electrophilic stress in HEK293T cells.<sup>18</sup> Furthermore, Akaike and co-workers demonstrated that CSE overexpression leads to increased intracellular levels of RSSH species in A549 cells, which confers resistance toward hydrogen peroxide (H<sub>2</sub>O<sub>2</sub>)-mediated oxidative stress.<sup>7</sup>

Interestingly, unlike RSH, RSSH in the protonated state are electrophilic and can react with nucleophiles, including RSH. The electrophilic properties of RSSH may result in nucleophilic attack by protein thiols (PSH) giving rise to generation of protein hydropersulfides (PSSH). In fact, this transformation has been proposed to protect protein thiols from irreversible modification during oxidative and/or electrophilic insult.<sup>11</sup> Consistent with this hypothesis, Greiner and co-workers demonstrated that the phosphatase and tensin homolog (PTEN) is protected from irreversible H<sub>2</sub>O<sub>2</sub>-mediated inhibition when the protein is in the PSSH form.<sup>19</sup> Accumulating evidence suggests that the electrophilic nature of RSSH serves to regulate redox signaling and contribute to various cellular functions.<sup>20</sup>

<sup>a</sup>Department of Chemistry, Johns Hopkins University, Baltimore, Maryland, 21218, USA. E-mail: jtoscانو@jhu.edu

<sup>b</sup>Division of Cardiology, Johns Hopkins University School of Medicine, Baltimore, Maryland, 21205, USA

<sup>c</sup>Department of Biomedical Sciences, University of Padova, Padova, Italy

† Electronic supplementary information (ESI) available. See DOI: 10.1039/d1sc01550h

‡ These authors contributed equally.





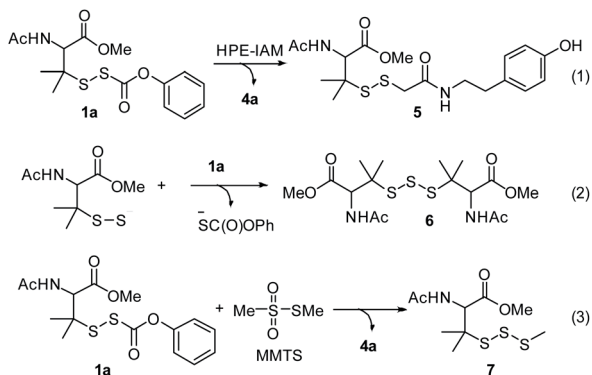
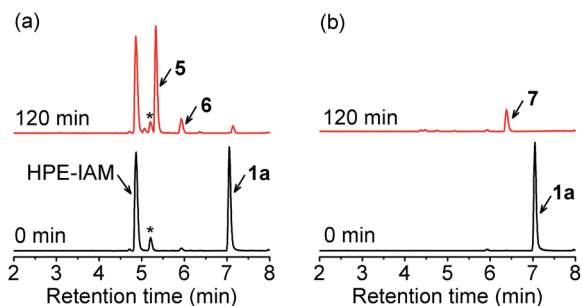
Scheme 3 RSSH generation from precursor **1a**.

Fig. 1 UPLC-MS traces showing RSSH generation from **1a** (100  $\mu\text{M}$ ) in the presence of (a) HPE-IAM (1 mM), and (b) MMTS (1 mM) in ammonium bicarbonate buffer (pH 7.4, 50 mM) containing the metal chelator diethylenetriaminepentaacetic acid (DTPA) (100  $\mu\text{M}$ ) at 37  $^{\circ}\text{C}$ . Asterisk indicates the presence of an impurity in the commercial HPE-IAM sample.

(MMTS). MMTS has been reported as an alkylating reagent for identification of small molecule and protein hydroperoxides.<sup>31,37</sup> Incubation of **1a** with 10 equiv. of MMTS shows RSS-S-Me **7** formation with no evidence of dialkyl trisulfide **6** (Fig. 1b and S4<sup>†</sup>), supporting that MMTS is a more efficient trap than HPE-IAM.

After confirming RSSH generation from **1a**, we analyzed the kinetics of RSSH release from alkylsulfenyl thiocarbonates in the presence of MMTS by high-performance liquid chromatography (HPLC). Due to the lack of a chromophore in MMTS adduct **7**, we monitored the decay of the RSSH precursor and formation of the corresponding phenol byproduct. First-order rate constants were obtained by plotting the precursor decay and phenol byproduct formation as a function of time. HPLC analysis of **1a** incubation with 10 equiv. of MMTS in phosphate buffered saline (PBS, pH 7.4, 100 mM) shows disappearance of **1a** ( $k = 5.39 \times 10^{-3} \text{ min}^{-1}$ ;  $t_{1/2} = 129 \pm 2 \text{ min}$ ) with concomitant formation of phenol ( $k = 5.33 \times 10^{-3} \text{ min}^{-1}$ ;  $t_{1/2} = 130 \pm 1 \text{ min}$ ) (Fig. 2). The observation of similar rate constants for both **1a** decay and phenol (**4a**) formation indicates a rapid reaction of released RSSH with MMTS, and that these observed rate constants indicate the RSSH release rate. Importantly, 92% of the byproduct phenol **4a** is observed. In addition, we also examined the effect of pH on the kinetics of RSSH release. As

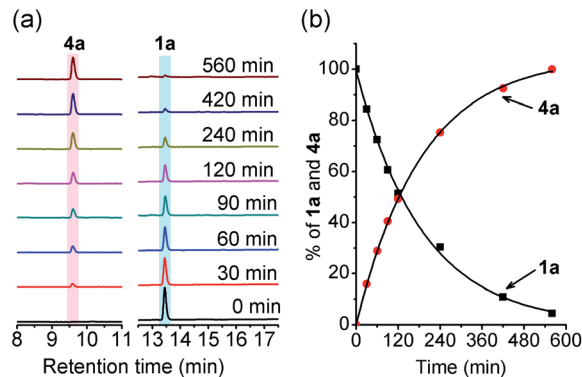


Fig. 2 (a) HPLC traces showing hydrolysis of **1a** (100  $\mu\text{M}$ ) in the presence of MMTS (1 mM) in PBS (pH 7.4, 100 mM) containing the metal chelator DTPA (100  $\mu\text{M}$ ) at 37  $^{\circ}\text{C}$ . An aliquot of the reaction mixture was withdrawn at the specified time and quenched with 0.1% formic acid. The decay of **1a** was monitored at 240 nm and formation of phenol **4a** at 275 nm. (b) Kinetics of **1a** decomposition and phenol **4a** formation. Data represent the average of three experiments. The curve is the calculated best fit to a single-exponential function.

expected, the rate of **1a** hydrolysis is enhanced at pH 8.0 ( $t_{1/2} = 37 \pm 3 \text{ min}$ ) and is slowed significantly at pH 6.0 ( $t_{1/2} = 1599 \pm 48 \text{ min}$ ), supporting the proposed base catalyzed hydrolysis to release RSSH.

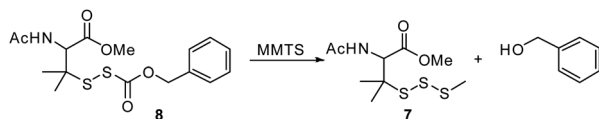
We then compared RSSH release kinetics for precursors containing a variety of *para*-substituted phenols. We hoped to decrease the rate of RSSH release through the introduction of electron-donating groups. Indeed, we observe a small decrease in the RSSH release rate from **1b**, equipped with a 4-Me substituent ( $137 \pm 4 \text{ min}$ ) (Table 1). Similarly, precursor **1c**, equipped with a 4-OMe substituent, shows a half-life  $147 \pm 2 \text{ min}$ , suggesting a minor effect of electron donating groups on RSSH release rate. As also expected, we find that electron withdrawing groups enhance the rate of RSSH release. For example, 4-F substituted precursor **1d** releases RSSH with a half-life of  $96 \pm 3 \text{ min}$ . Similarly, 4- $\text{CF}_3$  substituted precursor **1e**, and 4-CN substituted precursor **1f** generate RSSH with a half-life of  $56 \pm 3 \text{ min}$  and  $28 \pm 1 \text{ min}$ , respectively. Importantly, UPLC-MS analysis of **1a-f** following incubation with MMTS shows adduct **7** formation as the exclusive product (Fig. S5-S9<sup>†</sup>), and HPLC analysis confirms phenol byproduct **4a-f** formation in excellent

Table 1 Half-lives for precursors **1a-f** and phenol **4a-f** yields

Precursor	X	$t_{1/2}$ (min) <sup>a</sup>	ArOH	<b>4a-f</b> yield (%)
<b>1a</b>	4-H	$129 \pm 2$	<b>4a</b>	$92 \pm 2$
<b>1b</b>	4-CH <sub>3</sub>	$137 \pm 4$	<b>4b</b>	$93 \pm 4$
<b>1c</b>	4-OMe	$147 \pm 2$	<b>4c</b>	$92 \pm 1$
<b>1d</b>	4-F	$96 \pm 3$	<b>4d</b>	$96 \pm 6$
<b>1e</b>	4- $\text{CF}_3$	$56 \pm 3^b$	<b>4e</b>	$97 \pm 1$
<b>1f</b>	4-CN	$28 \pm 1$	<b>4f</b>	$97 \pm 2$

<sup>a</sup> RSSH precursors (100  $\mu\text{M}$ ) were incubated in the presence of MMTS (1 mM) in pH 7.4 PBS containing DTPA at 37  $^{\circ}\text{C}$ . <sup>b</sup> Reduced aqueous solubility required this experiment to be carried out in PBS with 50% acetonitrile. Reported data represent averages  $\pm$  SD ( $n = 3$ ).





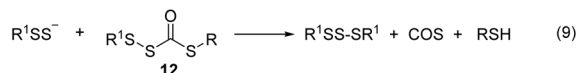
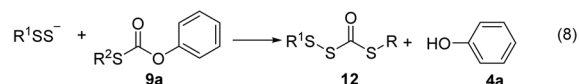
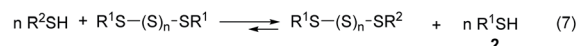
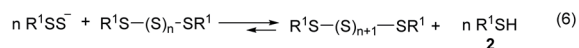
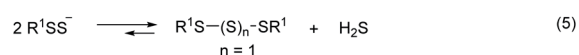
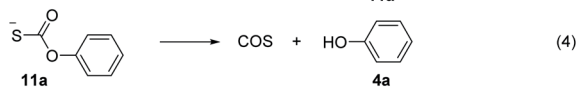
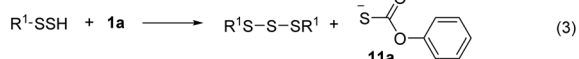
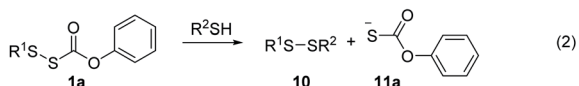
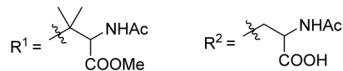
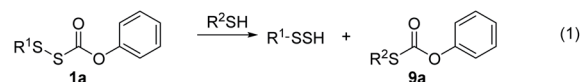
Scheme 4 RSSH generation from *O*-benzyl substituted RSSH precursor **8**.

yields (Table 1). Hammett analysis of the kinetic data of RSSH release from precursors **1a–f** indicates a  $\rho$  value of 0.71 (Fig. S47<sup>†</sup>), consistent with a mild substituents effect on the hydrolysis of these precursors. Taken together, these results indicate that the RSSH release kinetics of alkylsulfenyl thiocarbonates can be tuned through electronic modulation of the thiocarbonate carbonyl carbon in precursor **1**.

To further explore the substrate scope, we synthesized *O*-benzyl substituted RSSH precursor **8** (Scheme 4). Here, we observe significantly slower RSSH release ( $t_{1/2} = 2235 \pm 94$  min), indicating slow hydrolysis which is likely due to reduced electrophilicity of the thiocarbonate carbonyl carbon (*O*-benzyl substituent in **8** vs. *O*-phenyl in precursors **1a–f**).

### RSSH generation in the presence of thiol

Next, we examined the ability of alkylsulfenyl thiocarbonate **1a** to release RSSH in the presence of thiols. We anticipated that if thiol attacks at the carbonyl carbon of the thiocarbonate moiety,



Scheme 5 Proposed mechanism of RSSH and COS generation from **1a** in the presence of thiol.

we should observe RSSH and/or RSSH-derived polysulfides, along with *S*-alkyl-thiocarbonate **9a** (Scheme 5, eqn (1)). Alternatively, thiol can attack at the internal sulfur atom of the disulfide to produce unsymmetrical disulfide **10** and thiocarbonate intermediate **11a**, which can rapidly decompose to release COS and phenol (Scheme 5, eqn (2) and (4)). If formed, COS will be hydrolyzed to H<sub>2</sub>S in biological systems by the ubiquitous enzyme carbonic anhydrase (CA).<sup>38</sup>

Initially, the decomposition of **1a** was analyzed in the presence of 5 equiv. of *N*-acetylcysteine (NAC) in PBS (pH 7.4) by HPLC. Rapid decomposition of **1a** is observed in the presence of NAC ( $t_{1/2} = 0.64 \pm 0.11$  min) (ESI,† Table 3), indicating a rapid reaction between NAC and **1a**. To investigate the mechanism, we monitored this reaction by UPLC-MS. As shown in Fig. 3, disappearance of the peak attributed to **1a** is observed with concomitant formation of symmetrical dialkyl polysulfides (cyan highlight,  $\text{R}^1\text{SS}_n\text{SR}^1$ ,  $n = 1-4$ ), presumably formed by the decomposition of RSSH through disproportionation (Scheme 5, eqn (5) and (6)). Additionally, a small amount of unsymmetrical dialkyl polysulfide (pink highlight,  $\text{R}^1\text{SS}_n\text{SR}^2$ ,  $n = 0-3$ ) is observed, likely formed *via* NAC reaction with symmetrical dialkyl polysulfides (Scheme 5, eqn (7)). As expected, a new peak at 5.65 min corresponding to *N*-acetyl cysteine-thiocarbonate **9a** is also observed, confirming thiol attack at the perthiocarbonate carbonyl carbon of **1a** to release RSSH. Due to the unstable nature of RSSH under these experimental conditions, we measured the yield of the byproduct **9a** as an indication of RSSH yield. The observation of RSSH-derived polysulfides formation as major products led us to anticipate the efficient formation of byproduct **9a**. However, incubation of **1a** with 5 equiv. of *N*-acetylcysteine methyl ester shows only 53% formation of **9a**. The lower observed yield of **9a** is likely due to its further reaction with RSSH under these conditions. This hypothesis is supported by UPLC-MS data, where we observe appearance of a new

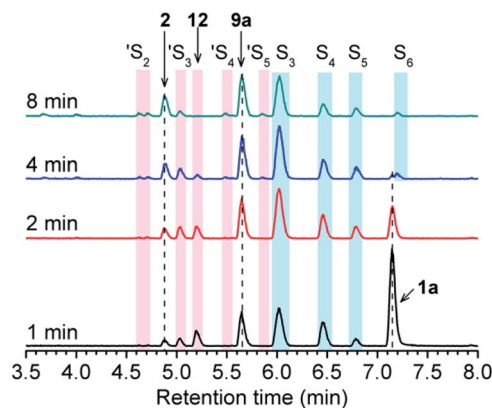
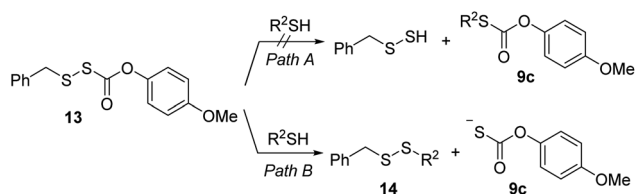


Fig. 3 UPLC-MS chromatograms of RSSH generation from **1a** (100  $\mu\text{M}$ ) in the presence of NAC (500  $\mu\text{M}$ ) in pH 7.4 ammonium bicarbonate (50 mM) containing the metal chelator DTPA (100  $\mu\text{M}$ ) at 37  $^\circ\text{C}$ . Aliquots taken at various times were quenched with 1% formic acid, and analyzed by UPLC-MS. RSSH-derived symmetrical dialkyl polysulfide, labeled as  $\text{S}_3$  to  $\text{S}_6$  ( $\text{R}^1\text{SS}_n\text{SR}^1$ ,  $n = 1-4$ , cyan highlight), and unsymmetrical dialkyl polysulfides labeled as  $\text{S}_2$  to  $\text{S}_5$  ( $\text{R}^1\text{SS}_n\text{SR}^2$ ,  $n = 0-3$ , pink highlight) formation is evident. A peak at 5.65 min attributed to thiocarbonate **9a** is also observed.



peak at 5.2 min with  $m/z = 427.0659$  (Fig. 3 and S12<sup>†</sup>). This peak is assigned to byproduct **12**, potentially formed by RSSH reaction with **9a** as shown in Scheme 5, eqn (8). Furthermore, disappearance of **12** is also observed, likely due to further reaction with RSSH producing dialkyl trisulfide and COS (Scheme 5, eqn (9)).

COS generation from **1a** was analyzed in the presence of NAC by membrane inlet mass-spectrometry (MIMS), a technique used for detection of dissolved hydrophobic gases in aqueous solutions.<sup>39,40</sup> For comparison, analogous experiments were conducted with the primary alkyl RSSH precursor **13** (Scheme 6). Thiol is expected to react with **13** selectively at the disulfide's internal sulfur atom due to its steric accessibility to produce unsymmetrical disulfide and thiocarbonate intermediate **9c**, which subsequently decomposes to release COS (Scheme 6 and Fig. S34<sup>†</sup>). Comparison of COS release from **1a** in the presence of NAC shows only approximately 20% COS production with respect to that observed for precursor **13** (Fig. 4a). Under these conditions, the observed COS signal is likely a result of both NAC and initially released RSSH reaction with **1a** to produce thiocarbonate intermediate **11a** (Scheme 5, eqn (2) and (3)). Taken together, these results demonstrate that **1a** predominantly produces RSSH, even in the presence of thiols. We also examined COS release from precursors **1b–f** in the presence of NAC. As shown in Fig. 4a, similar COS generation is observed for all precursors indicating electron donating/withdrawing groups do not have a major effect on COS release rates. The reactivity of these precursors toward GSH was also measured. As expected, a slightly faster COS release is observed in the presence of GSH ( $pK_a = 8.83$ ) compared with NAC ( $pK_a = 9.52$ ) (Fig. 4b), presumably due to a higher concentration of the glutathione thiolate under these conditions.



Scheme 6 Proposed Mechanism of **13** reaction with thiol.

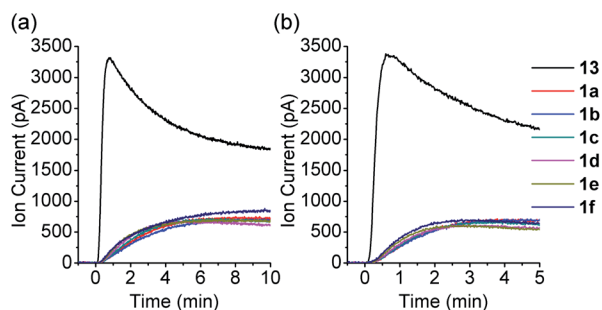
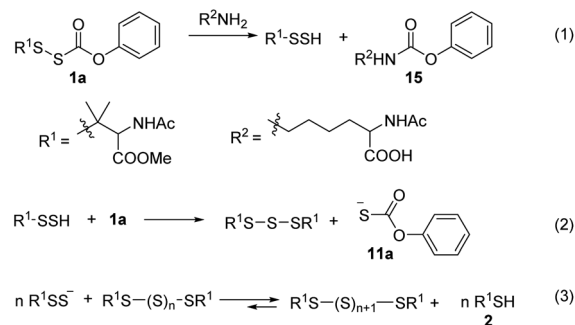


Fig. 4 COS MIMS signals at  $m/z = 60$  observed following the reaction of control compound **9** (50  $\mu M$ ) and RSSH precursors **1a–f** (50  $\mu M$ ) with (a) NAC, and (b) GSH (0.25 mM, 5 equiv.) in PBS (pH 7.4, 10 mM) with DTPA (100  $\mu M$ ) at 37  $^{\circ}C$ .



Scheme 7 Proposed Mechanism of **1a** reaction with amine.

Reaction of *O*-benzyl substituted precursor **8** with NAC was also examined. As expected, a rapid decomposition of **8** is observed in the presence of thiol ( $t_{1/2} = 4.0 \pm 0.7$  min vs. 2235 min in the absence of NAC). With respect to **1a**, **8** decomposes about six times slower in the presence of thiol. Similarly, slower COS generation is observed from precursor **8** in the presence of thiol compared to **1a** (Fig. S36<sup>†</sup>). We also examined whether the reduced electrophilicity of the carbonyl carbon of precursor **8** favors thiol attack at the disulfide, which would preclude RSSH generation. However, UPLC-MS analysis shows  $R^1SS_nSR^1$  ( $n = 1-4$ ) and  $R^1SS_nSR^2$  ( $n = 0-3$ ) formation (Fig. S23<sup>†</sup>), indicating that **8** releases RSSH even in the presence of thiol. Thus, the results presented here confirm that alkylsulfenyl thiocarbonate thiolysis can be achieved under physiological conditions to release RSSH.

### RSSH generation in the presence of amine

We tested the ability **1a** to release RSSH in the presence of amines. We anticipated that if amine attacks at the carbonyl carbon of the thiocarbonate moiety, we should observe RSSH and/or RSSH-derived polysulfides, along with alkyl-carbamate **15** (Scheme 7, eqn (1)). Incubation of **1a** with *L*-lysine (5 equiv.) shows disappearance of the peak attributed to **1a** with

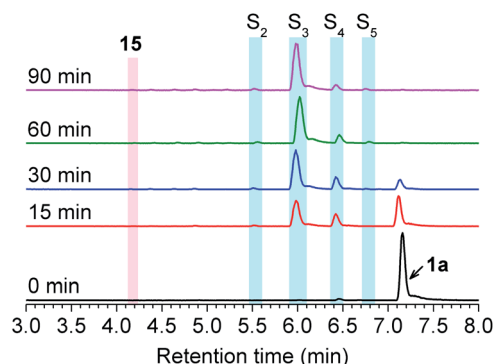


Fig. 5 UPLC-MS chromatograms of RSSH generation from **1a** (100  $\mu M$ ) in the presence of lysine (500  $\mu M$ ) in pH 7.4 ammonium bicarbonate (50 mM) containing the metal chelator DTPA (100  $\mu M$ ) at 37  $^{\circ}C$ . Aliquots taken at various times were quenched with 1% formic acid and analyzed by UPLC-MS. RSSH-derived symmetrical dialkyl polysulfide, labeled as  $S_2$  to  $S_5$  ( $R^1SS_nSR^1$ ,  $n = 0-3$ , cyan highlight), formation is evident. The very minor peak at 4.17 min corresponds to carbamate **15**.



concomitant formation of symmetrical dialkyl polysulfides (Fig. 5). However, only a very minor peak corresponding to expected byproduct **15** is observed, suggesting that RSSH release from **1a** is mainly *via* hydrolysis even in the presence of amine.

### RSSH protection against oxidative stress

Oxidative stress has been implicated in the etiologies of many cardiovascular diseases.<sup>41,42</sup> Oxidative stress usually arises from overproduction of reactive oxygen species (ROS). ROS constitutes both oxygen free radicals, such as superoxide, hydroxyl radicals, and peroxy radicals, and non-radicals, such as hydrogen peroxide, and hypochlorous acid. It has been proposed that RSSH generation can be an endogenous cellular protectant in response to oxidative stress.<sup>17</sup> Furthermore, it appears likely that the proposed mechanism of protection can be augmented pharmacologically with the addition of RSSH donor species.

To test this hypothesis, we evaluated RSSH-mediated cellular protection against oxidative-stress. First, we examined the cytotoxicity of **1a** on H9c2 cardiac myoblasts using the Sytox viability assay, which measures cell membrane integrity.<sup>43</sup> Both precursor **1a** and its byproduct phenol show no toxicity toward H9c2 cells up to 100  $\mu\text{M}$  (Fig. S43<sup>†</sup>). We then measured the cytoprotective effects of **1a** against oxidative stress. As expected, treatment of H9c2 cells with hydrogen peroxide (200  $\mu\text{M}$ ) results in reduced cell viability (Fig. 6a), measured using the CCK-8 viability assay, which measures cellular reducing capacity. Interestingly, pre-treating myoblasts with precursor **1a** for 4 h results in a dose-dependent decrease of  $\text{H}_2\text{O}_2$ -induced toxicity (Fig. 6a). Remarkably, pre-treatment with only 5  $\mu\text{M}$  **1a** for 8 h also shows protection against 200  $\mu\text{M}$  of  $\text{H}_2\text{O}_2$ , demonstrating the potency of these newly developed alkylsulfenyl thiocarbonate RSSH precursors against oxidative stress. Under similar conditions, the phenol byproduct shows no protective effect against  $\text{H}_2\text{O}_2$ -mediated toxicity, indicating that the protection is due to RSSH. In addition, we have measured the protective effects of thiol **2** in H9c2 cells. This thiol does indeed show some protection against  $\text{H}_2\text{O}_2$ -mediated toxicity, but to a much

lesser extent compared with **1a** (Fig. S44<sup>†</sup>), indicating important role of RSSH in cytoprotection against oxidative stress. The cytoprotective effect of **1a** was also independently measured using the Sytox viability assay due to the potential background reduction of CCK-8 by reactive sulfur species leading to artifactual viability measurements.<sup>44</sup> As shown in Fig. 6b, **1a** consistently shows protective effects against  $\text{H}_2\text{O}_2$ -mediated toxicity. The protective effects against oxidative stress warrant future investigation as the potency of **1a** suggests cytoprotective properties beyond direct scavenging of free-radical products derived from  $\text{H}_2\text{O}_2$ . Taken together, these results demonstrate the potential therapeutic benefit of RSSH donors in the context of oxidative stress and suggest that precursors that increase intracellular RSSH levels are potentially useful agents against oxidative stress-induced diseases.

### Intracellular RSSH release

We also tested for increased intracellular RSSH levels resulting from incubation with **1a** utilizing SSP4, a fluorescent probe that has been used to detect of intracellular sulfane sulfur.<sup>45,46</sup> Sulfane sulfur refers to a sulfur atom with six valence electrons and no charge. Biologically important sulfane sulfur compounds include RSSH, polysulfides ( $\text{RS}_n\text{SH}$  or  $\text{RSS}_n\text{SR}$ ,  $n \geq 1$ ), inorganic polysulfides ( $\text{HSS}_n\text{H}$ ,  $n \geq 1$ ), and elemental sulfur ( $\text{S}_8$ ). Briefly, cells were incubated with SSP4 in the presence of cetrimonium bromide (CTAB) for 20 min and then washed with serum-free media before **1a** is introduced. We did not observe a significant increase of the SSP4 fluorescence signal following treatment with 50  $\mu\text{M}$  **1a** due to the low amount of RSSH released at this concentration falling below the detection limit of the probe (Fig. 7). However, dose-dependent increases in fluorescence intensity are observed for 100 and 200  $\mu\text{M}$  **1a** over a period of 3 h. Since the SSP4 probe is known to react with a variety of sulfane sulfur species, the fluorescence signal observed upon

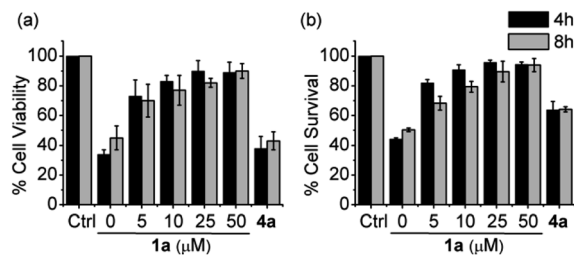


Fig. 6 Cell viability of H9c2 cardiac myoblasts pretreated with RSSH precursor **1a** at 0, 5, 10, 25, and 50  $\mu\text{M}$  and the byproduct phenol **4a** at 50  $\mu\text{M}$  for 4 and 8 h followed by exposure to  $\text{H}_2\text{O}_2$  (200  $\mu\text{M}$ ) for 2 h. (a) Quantification of viability was carried out using Cell Counting Kit-8 (CCK-8). Results are expressed as the mean  $\pm$  SEM ( $n = 5$  for each treatment group) with three independent experiments. (b) Quantification of cytotoxicity was carried out using Sytox green nucleic acid stain. Results are expressed as the mean  $\pm$  SEM ( $n = 5$  for each treatment group) with five independent experiments.

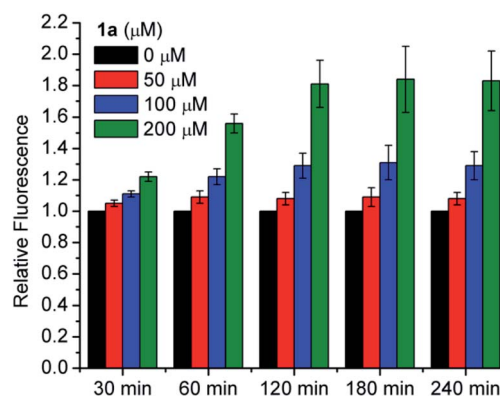


Fig. 7 Intracellular RSSH release in H9c2 cardiac myoblasts. H9c2 cells were pretreated with SSP4 (20  $\mu\text{M}$ ) and CTAB (500  $\mu\text{M}$ ) for 20 min, followed by incubation with RSSH precursor **1a** at 0, 50, 100, 25, and 200  $\mu\text{M}$ . Fluorescence intensity was measured at the indicated times using a plate reader at the excitation and emission wavelengths of 482 nm and 515 nm, respectively. Results are normalized to the 0  $\mu\text{M}$  value at each time point and expressed as the mean  $\pm$  SEM ( $n = 3$  for each treatment group) with three independent experiments.



treatment of **1a** is likely due to RSSH and/or other sulfane sulfur species that might be present in the equilibrium with RSSH (e.g., Scheme 5). We measured the sulfane sulfur in H9c2 cells treated with *N*-acetyl *O*-methyl cysteine trisulfide (*N*-Ac-OMe-Cys-(S)<sub>3</sub>) using the SSP4 probe and find that a higher fluorescence signal for *N*-Ac-OMe-Cys-(S)<sub>3</sub> compared with **1a** (Fig. S45†). However, sulfane sulfur detection under cell-free conditions also shows a much higher fluorescence signal intensity for Na<sub>2</sub>S<sub>3</sub> and *N*-Ac-OMe-Cys-(S)<sub>3</sub> compared with **1a** (Fig. S46†). Based on these data we believe that **1a** efficiently generates RSSH intracellularly, but reduced reactivity of the **1a**-derived sterically hindered RSSH and/or dialkyl polysulfides towards SSP4 probe likely contributes to the observed lower fluorescence intensity. Thus, we conclude that the cytoprotective effects of **1a** are attributed to increasing sulfane sulfur pools within the cultured cells.

## Conclusions

This study reports a new strategy for efficient RSSH generation based on the hydrolysis of alkylsulfenyl thiocarbonates under physiologically relevant conditions. We demonstrate that RSSH generation from these precursors can be tuned by modifying the thiocarbonate carbonyl group's electrophilicity. These alkylsulfenyl thiocarbonates also generate RSSH in the presence of thiol. As a proof-of-principle of possible protective effects associated with RSSH, we have demonstrated the potential benefit of these donors in the context of oxidative stress in H9c2 cardiac myoblasts. Furthermore, these precursors also increase intracellular sulfane sulfur levels in H9c2 cells. We hope that this series of RSSH precursors may be used as a research tool for delineating RSSH cell signaling mechanisms.

## Author contributions

V. S. K carried out the synthesis, collected the spectral data, and performed UPLC-MS-based assays. S. C. A. performed the HPLC analysis to measure the kinetics of RSSH release. B. M. P performed the cell toxicity experiments, and intracellular sulfane sulfur analysis. J. P. T. and N. P. contributed to the conceptualization, discussion, manuscript writing, review, and editing.

## Conflicts of interest

The authors declare that there is no conflict of interests.

## Acknowledgements

We gratefully acknowledge the National Science Foundation (CHE-1900285 to J.P.T.) and the National Institutes of Health (T32 GM080189 for support of B.M.P. and R01 HL136918 to N.P.) for generous support for this research. We also thank Drs Christopher McGinity (National Cancer Institute) and Jon Fukuto (Sonoma State University) for advice on intracellular RSSH detection.

## Notes and references

- 1 L. Zhang, Y. Wang, Y. Li, L. Li, S. Xu, X. Feng and S. Liu, *Front. Pharmacol.*, 2018, **9**, 1066.
- 2 H. Kimura, *Molecules*, 2014, **19**, 16146–16157.
- 3 L. A. Barr and J. W. Calvert, *Circ. J.*, 2014, **78**, 2111–2118.
- 4 J. M. Fukuto, L. J. Ignarro, P. Nagy, D. A. Wink, C. G. Kevil, M. Feelisch, M. M. Cortese-Krott, C. L. Bianco, Y. Kumagai, A. J. Hobbs, J. Lin, T. Ida and T. Akaike, *FEBS Lett.*, 2018, **592**, 2140–2152.
- 5 M. R. Filipovic, J. Zivanovic, B. Alvarez and R. Banerjee, *Chem. Rev.*, 2018, **118**, 1253–1337.
- 6 A. K. Mustafa, M. M. Gadalla, N. Sen, S. Kim, W. Mu, S. K. Gazi, R. K. Barrow, G. Yang, R. Wang and S. H. Snyder, *Sci. Signaling*, 2009, **2**, ra72.
- 7 T. Ida, T. Sawa, H. Ihara, Y. Tsuchiya, Y. Watanabe, Y. Kumagai, M. Suematsu, H. Motohashi, S. Fujii, T. Matsunaga, M. Yamamoto, K. Ono, N. O. Devarie-Baez, M. Xian, J. M. Fukuto and T. Akaike, *Proc. Natl. Acad. Sci. U. S. A.*, 2014, **111**, 7606–7611.
- 8 H. Kunikata, T. Ida, K. Sato, N. Aizawa, T. Sawa, H. Tawarayama, N. Murayama, S. Fujii, T. Akaike and T. Nakazawa, *Sci. Rep.*, 2017, **7**, 41984.
- 9 É. Dóka, I. Pader, A. Bíró, K. Johansson, Q. Cheng, K. Ballagó, J. R. Prigge, D. Pastor-Flores, T. P. Dick, E. E. Schmidt, E. S. J. Arnér and P. Nagy, *Sci. Adv.*, 2016, **2**, e1500968.
- 10 S. Longen, F. Richter, Y. Köhler, I. Wittig, K.-F. Beck and J. Pfeilschifter, *Sci. Rep.*, 2016, **6**, 29808.
- 11 J. M. Fukuto, J. Lin, V. S. Khodade and J. P. Toscano, *Antioxid. Redox Signaling*, 2020, **33**, 1295–1307.
- 12 P. K. Yadav, M. Martinov, V. Vitvitsky, J. Seravalli, R. Wedmann, M. R. Filipovic and R. Banerjee, *J. Am. Chem. Soc.*, 2016, **138**, 289–299.
- 13 T. Akaike, T. Ida, F.-Y. Wei, M. Nishida, Y. Kumagai, M. M. Alam, H. Ihara, T. Sawa, T. Matsunaga, S. Kasamatsu, A. Nishimura, M. Morita, K. Tomizawa, A. Nishimura, S. Watanabe, K. Inaba, H. Shima, N. Tanuma, M. Jung, S. Fujii, Y. Watanabe, M. Ohmuraya, P. Nagy, M. Feelisch, J. M. Fukuto and H. Motohashi, *Nat. Commun.*, 2017, **8**, 1177.
- 14 E. Cuevasanta, M. Lange, J. Bonanata, E. L. Coitiño, G. Ferrer-Sueta, M. R. Filipovic and B. Alvarez, *J. Biol. Chem.*, 2015, **290**, 26866–26880.
- 15 D. Benchoam, J. A. Semelak, E. Cuevasanta, M. Mastrogiovanni, J. S. Grassano, G. Ferrer-Sueta, A. Zeida, M. Trujillo, M. N. Möller, D. A. Estrin and B. Alvarez, *J. Biol. Chem.*, 2020, **295**, 15466–15481.
- 16 J. Zarenkiewicz, V. S. Khodade and J. P. Toscano, *J. Org. Chem.*, 2021, **86**, 868–877.
- 17 L. Álvarez, C. L. Bianco, J. P. Toscano, J. Lin, T. Akaike and J. M. Fukuto, *Antioxid. Redox Signaling*, 2017, **27**, 622–633.
- 18 C. L. Bianco, T. Akaike, T. Ida, P. Nagy, V. Bogdandi, J. P. Toscano, Y. Kumagai, C. F. Henderson, R. N. Goddu, J. Lin and J. M. Fukuto, *Br. J. Pharmacol.*, 2019, **176**, 671–683.
- 19 R. Greiner, Z. Pálkás, K. Bäsell, D. Becher, H. Antelmann, P. Nagy and T. P. Dick, *Antioxid. Redox Signaling*, 2013, **19**, 1749–1765.



- 20 S. Kasamatsu, A. Nishimura, M. Morita, T. Matsunaga, H. Abdul Hamid and T. Akaike, *Molecules*, 2016, **21**.
- 21 S. Koike, S. Nishimoto and Y. Ogasawara, *Redox Biol.*, 2017, **12**, 530–539.
- 22 C.-t. Yang, N. O. Devarie-Baez, A. Hamsath, X.-d. Fu and M. Xian, *Antioxid. Redox Signaling*, 2019, **33**, 1092–1114.
- 23 P. Bora, P. Chauhan, S. Manna and H. Chakrapani, *Org. Lett.*, 2018, **20**, 7916–7920.
- 24 Y. Wang, K. M. Dillon, Z. Li, E. W. Winckler and J. B. Matson, *Angew. Chem., Int. Ed.*, 2020, **59**, 16698–16704.
- 25 C. R. Powell, K. M. Dillon, Y. Wang, R. J. Carrazzone and J. B. Matson, *Angew. Chem., Int. Ed.*, 2018, **57**, 6324–6328.
- 26 J. Kang, S. Xu, M. N. Radford, W. Zhang, S. S. Kelly, J. J. Day and M. Xian, *Angew. Chem., Int. Ed.*, 2018, **57**, 5893–5897.
- 27 I. Artaud and E. Galardon, *ChemBioChem*, 2014, **15**, 2361–2364.
- 28 V. S. Khodade and J. P. Toscano, *J. Am. Chem. Soc.*, 2018, **140**, 17333–17337.
- 29 V. S. Khodade, B. M. Pharoah, N. Paolucci and J. P. Toscano, *J. Am. Chem. Soc.*, 2020, **142**, 4309–4316.
- 30 A. Chaudhuri, Y. Venkatesh, J. Das, M. Gangopadhyay, T. K. Maiti and N. D. P. Singh, *J. Org. Chem.*, 2019, **84**, 11441–11449.
- 31 Y. Zheng, B. Yu, Z. Li, Z. Yuan, C. L. Organ, R. K. Trivedi, S. Wang, D. J. Lefer and B. Wang, *Angew. Chem., Int. Ed.*, 2017, **56**, 11749–11753.
- 32 Z. Yuan, Y. Zheng, B. Yu, S. Wang, X. Yang and B. Wang, *Org. Lett.*, 2018, **20**, 6364–6367.
- 33 S. J. Brois, J. F. Pilot and H. W. Barnum, *J. Am. Chem. Soc.*, 1970, **92**, 7629–7631.
- 34 Y. Zhao, M. M. Cerda and M. D. Pluth, *Chem. Sci.*, 2019, **10**, 1873–1878.
- 35 D. N. Harpp and A. Granata, *Tetrahedron Lett.*, 1976, **17**, 3001–3004.
- 36 D. N. Harpp and A. Granata, *J. Org. Chem.*, 1979, **44**, 4144–4148.
- 37 J. Pan and K. S. Carroll, *ACS Chem. Biol.*, 2013, **8**, 1110–1116.
- 38 C. P. Chengelis and R. A. Neal, *Toxicol. Appl. Pharmacol.*, 1980, **55**, 198–202.
- 39 G. Hoch and B. Kok, *Arch. Biochem. Biophys.*, 1963, **101**, 160–170.
- 40 M. R. Cline, C. Tu, D. N. Silverman and J. P. Toscano, *Free Radical Biol. Med.*, 2011, **50**, 1274–1279.
- 41 N. S. Dhalla, R. M. Temsah and T. Netticadan, *J. Hypertens.*, 2000, **18**, 655–673.
- 42 R. D’Oria, R. Schipani, A. Leonardini, A. Natalicchio, S. Perrini, A. Cignarelli, L. Laviola and F. Giorgino, *Oxid. Med. Cell. Longevity*, 2020, **2020**, 5732956.
- 43 L. J. Jones and V. L. Singer, *Anal. Biochem.*, 2001, **293**, 8–15.
- 44 H. Tominaga, M. Ishiyama, F. Ohseto, K. Sasamoto, T. Hamamoto, K. Suzuki and M. Watanabe, *Anal. Commun.*, 1999, **36**, 47–50.
- 45 W. Chen, C. Liu, B. Peng, Y. Zhao, A. Pacheco and M. Xian, *Chem. Sci.*, 2013, **4**, 2892–2896.
- 46 E. Marutani, M. Sakaguchi, W. Chen, K. Sasakura, J. Liu, M. Xian, K. Hanaoka, T. Nagano and F. Ichinose, *MedChemComm*, 2014, **5**, 1577–1583.

